Inorg. Chem. **2007**, *46*, 409–416

Electrochemical and Photophysical Properties of DNA Metallo-intercalators Containing the Ruthenium(II) Tris(1-pyrazolyl)methane Unit

Simon P. Foxon, Clive Metcalfe, Harry Adams, Michelle Webb, and Jim A. Thomas*

Department of Chemistry, University of Sheffield, Sheffield, U.K. S3 7HF

Received April 27, 2006

Three new ruthenium(II) complexes containing the tris(1-pyrazolyl)methane (tpm) ligand have been prepared: [Ru(tpm)(L)(dppn)]$^{n+}$ (where $n = 1$; L = Cl (**5**), $n = 2$; L = MeCN (**6**) and pyridine (**7**); dppn = benzo[*i*]dipyrido[3,2-*a*:2′,3′-*c*]phenazine). Complex **6** was structurally characterized by single-crystal X-ray diffraction. Binding parameters of these complexes with calf thymus DNA are reported and compared to those obtained for a previously reported monocation, [RuCl(tpm)(dppz)]$^+$. Binding studies with the dications and the synthetic oligonucleotides poly(dA)·poly(dT) and poly(dG)·poly(dC) have also been determined. Photophysical and electrochemical properties of **5**–**7** have been investigated and compared with their dipyridophenazine (dppz) analogues.

Introduction

The DNA binding properties of [Ru(phen)$_2$(dppz)]$^{2+}$ (**1**) (phen = 1,10-phenanthroline, dppz = dipyrido[3,2-*a*:2′,3′-*c*]phenazine) (see Figure 1) have attracted particular attention.[1−5] Although the exact orientation of the complex when bound to DNA has been open to much discussion, it is widely accepted that intercalation of the dppz ligand into the DNA base stack forms the basis of interaction.[1−4,6] The DNA binding process can be monitored using UV−visible spectroscopy, as intercalation results in large hypochromic shifts in the absorption bands of the complex.[2,4,7−13] Luminescence offers a further means of monitoring binding in what has become known as the DNA "light switch" effect: emission from aqueous solutions of **1** is quenched by water molecules, while binding to DNA enhances luminescence by several orders of magnitude.[1,6,14,15]

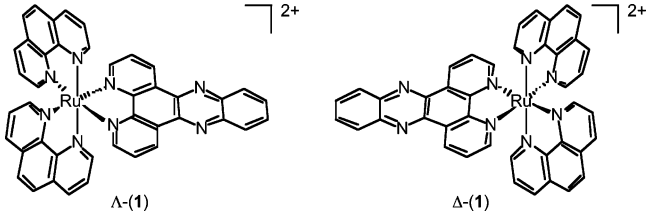

Figure 1. Enantiomers of [Ru(phen)$_2$(dppz)]$^{2+}$.

1 and its derivatives are synthesized as racemic mixtures—Figure 1. Although the Λ and Δ enantiomers can be resolved via classical or chromatographic procedures, they show only modest enantioselective DNA binding.[2,11] Furthermore, the resolved ruthenium(II) center in such complexes is coordinately saturated and attempts to extend the system often involves nontrivial modification of the coordinated aromatic ligands.[2,12,13] To address the issues outlined above, we have been investigating the properties of *achiral* [Ru(tpm)(L)(dppz)]$^{n+}$ complexes[5,16] (tpm = tris(1-pyrazolyl)methane, L = chloride, *N*-donor ligand, $n = 1, 2$), which contain an easily modulated coordination site (**2**−**4**) (see Figure 2).

* To whom correspondence should be addressed. Fax: +44 (0)114 273 8673. Tel: +44 (0)114 222 9325. E-mail: james.thomas@sheffield.ac.uk.

(1) Friedman, A. E.; Chambron, J.-C.; Sauvage, J.-P.; Turro, N. J.; Barton, J. K. *J. Am. Chem. Soc.* **1990**, *112*, 4960.
(2) Hiort, C.; Lincoln, P.; Nordén, B. *J. Am. Chem. Soc.* **1993**, *115*, 3448.
(3) Tuite, E.; Lincoln, P.; Nordén, B. *J. Am. Chem. Soc.* **1997**, *119*, 239.
(4) Holmlin, R. E.; Stemp, E. D. A.; Barton, J. K. *Inorg. Chem.* **1998**, *37*, 29.
(5) Metcalfe, C.; Thomas, J. A. *Chem. Soc. Rev.* **2003**, *215*.
(6) Jenkins, Y.; Friedman, A. E.; Turro, N. J.; Barton, J. K. *Biochemistry* **1992**, *31*, 10809.
(7) Erkkila, K. E.; Odom, D. T.; Barton, J. K. *Chem. Rev.* **1999**, *99*, 2777.
(8) Yam, V. W.-W.; Lo, K. K.-W.; Cheung, K.-K.; Kong, R. Y.-C. *J. Chem. Soc., Dalton Trans.* **1997**, *2067*.
(9) Kielkopf, C. L.; Erkkila, K. E.; Hudson, B. P.; Barton, J. K.; Rees, D. C. *Nature Struct. Biol.* **2000**, *7*, 117.
(10) Carson, D. L.; Huchital, D. H.; Mantilla, E. J.; Sheardy, R. D.; Murphy, W. R., Jr. *J. Am. Chem. Soc.* **1993**, *115*, 6424.
(11) Haq, I.; Lincoln, P.; Suh, D.; Nordén, B.; Chowdrey, B. Z.; Chaires, J. B. *J. Am. Chem. Soc.* **1995**, *117*, 4788.
(12) Önfelt, B.; Lincoln, P.; Nordén, B. *J. Am. Chem. Soc.* **2001**, *123*, 3630.
(13) Lincoln, P.; Nordén, B. *Chem. Commun.* **1996**, *2145*.
(14) Friedman, A. E.; Kumar, C. V.; Turro, N. J.; Barton, J. K. *Nucleic Acid Res.* **1991**, *19*, 2595.
(15) Hartshorn, R. M.; Barton, J. K. *J. Am. Chem. Soc.* **1992**, *114*, 5919.
(16) Metcalfe, C.; Adams, H.; Haq, I.; Thomas, J. A. *Chem. Commun.* **2003**, *1152*.

10.1021/ic0607134 CCC: $37.00
Published on Web 12/16/2006

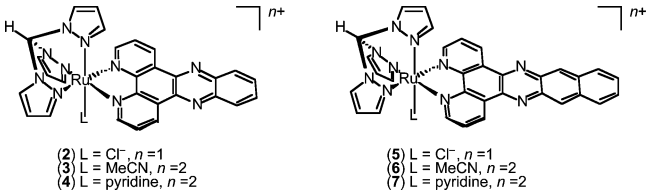

Figure 2. Ruthenium(II) tris(1-pyrazolyl)methane complexes relevant to this study.

Initial work using monometallic complex **2** as a precursor to synthesize **3** and **4** has shown that the DNA binding parameters of the latter two complexes compare favorably with those of **1**, and moreover, complex **4** was found to have a binding preference for GC sequences of DNA.[5]

We now report further on the biophysical and photophysical properties of these complexes. Furthermore, to investigate the effect of extending the length of the intercalative moiety in such systems, we have prepared three new complexes: $[Ru(tpm)(Cl)(dppn)]^+$ (**5**), $[Ru(tpm)(MeCN)(dppn)]^{2+}$ (**6**), and $[Ru(tpm)(py)(dppn)]^{2+}$ (**7**) (where dppn = benzo[*i*]-dipyrido[3,2-*a*:2′,3′-*c*]phenazine), see Figure 2. We were also motivated by the fact that there are very few characterized complexes containing the dppn ligand—surprising considering its structural similarity to the more widely employed dppz ligand.

Barton et al. prepared a family of substituted dppz ligands, one of which was $[Ru(phen)_2(dppn)]^{2+}$, in order to explore how the structure and nature of the substituted dppz ligand affected the luminescence properties in the absence and presence of DNA.[15] However, none of the ruthenium(II) complexes prepared containing modified dppz ligands displayed "light switch" effects comparable to the parent complex $[Ru(phen)_2(dppz)]^{2+}$. Nordén et al. studied the ligand size effect of three complexes of $[Ru(phen)_2(L)]^{2+}$ (where L = phen, dppz, and dppn) on third strand stabilization with poly(dT*dA−dT) triplex.[17] They concluded that all the complexes bind from the minor groove of the triplex with the dppz and dppn ligands intercalated. Third strand stabilization was dependent on L, increasing in the order phen < dppz < dppn. Yam et al. structurally characterized a rhenium(I) complex of dppn and reported its DNA binding properties and photocleavage activity of plasmid DNA.[8] They found that the intrinsic binding constant (K_b) for the interaction of $[(CO)_3Re(dppn)(py)]^+$ with calf thymus DNA (CT-DNA) was very similar to that obtained for $[(CO)_3Re(dppz)(py)]^+$ ($K_b = 4 \times 10^4$ dm^3 mol^{-1}).

Herein we describe and compare the photophysical properties of the dppn-based systems and the DNA-binding studies of **6** and **7**, with respect to complexes **2**−**4**, with CT-DNA, poly(dA)·poly(dT), and poly(dG)·poly(dC). As far as we are aware, this study represents the first quantitative investigation of the binding parameters of ruthenium(II) complexes of dppn with CT-DNA and synthetic oligonucleotides. We also report the first structurally characterized ruthenium(II) complex containing the dppn ligand.

(17) Ardhammar, M.; Lincoln, P.; Nordén, B. *J. Phys. Chem. B* **2001**, *105*, 11363.

Experimental Section

Materials. Solvents were dried and purified using standard literature methods, while other commercially available materials were used as received. Phenanthroline-5,6-dione,[18,19] tpm,[20] (tpm)-$RuCl_3 \cdot 3H_2O$,[21] and dppn[22] were synthesized via literature methods. Complexes **2**−**4** were prepared as described previously.[5,21] The buffer used for UV−visible titrations consisted of 25 mM NaCl and 5 mM tris (pH 7.0) made with doubly distilled water (Millipore). CT-DNA was purchased from Sigma and was purified until $A_{260}/A_{280} > 1.9$. Concentrations of CT-DNA solutions were determined spectroscopically using the extinction coefficient of CT-DNA ($\epsilon = 6600$ dm^3 mol^{-1} cm^{-1} at 260 nm). Poly(dA)·poly(dT) and poly(dG)·poly(dC) homopolymers were purchased from Pharmacia Biotech Ltd. and were used as received. Each sample was dissolved in the above buffer (2 cm^3) and then placed in dialysis tubing. The samples were dialyzed for at least 24 h. The concentrations of the homopolymers were determined by UV−visible spectroscopy using the following λ_{max}(tris buffer)/nm (ϵ/dm^3 mol^{-1} cm^{-1}): poly(dA)·poly(dT), 260 (6000); poly(dG)·poly(dC), 253 (7400).

Instrumentation. Standard ^{1}H NMR spectra were recorded on a Bruker AM250 machine. FAB mass spectra were obtained on a Kratos MS80 machine working in positive-ion mode, with *m*-nitrobenzyl alcohol matrix. UV−visible spectra were recorded on a Unicam UV2 spectrometer or Cary 50 spectrometer in twin-beam mode. Spectra were recorded in matched quartz cells and were baseline-corrected. Steady-state luminescence emission spectra were recorded either in aerated acetonitrile or tris buffer solutions on a Hitachi F-4500 instrument. Luminescence lifetimes were acquired on an Edinburgh Instruments mini-τ spectrometer (410 nm excitation wavelength, 75 ps pulse width) operating under time-correlated single-photon counting conditions. Cyclic voltammograms were recorded using an EG&G model Versastat II potentiostat and the EG&G electrochemistry power suite software package. Potentials were measured against a Ag/AgCl reference electrode, and ferrocene was used as an internal reference. Viscosity measurements were performed on a Cannon−Manning semi-micro viscometer (size 50) immersed in a thermostatted bath maintained at 27.0 °C

DNA Titration Protocol. DNA binding parameters of **2**−**4** have been determined previously (see Table 6 below).[5] Complexes **6** and **7** were converted to their chloride salts by reaction with [*n*Bu$_4$N]Cl in acetone. A 100 μM complex stock solution in tris buffer (100 μL) was then diluted into tris buffer (3 cm^3) (in a 1 cm path length optical glass cuvette maintained at 25 °C) to give a final complex concentration of ca. 15 μM. Tris buffer (3 cm^3) was loaded into another identical cuvette and placed in the reference cell of the spectrometer. Both the sample and the reference cells were mixed 30 times with a Gilson P1000 pipet. After 30 min to allow the cells to equilibrate, the first spectrum was recorded between 700 and 200 nm. DNA solution (2−5 μL) was then added to both the sample and reference cell followed by a further 30 times mixing. The spectrum was taken again, this time showing a hypsochromic shift indicating the formation of a metal complex−DNA interaction. The titration process was repeated until there was

(18) Paw, W.; Eisenberg, R. *Inorg. Chem.* **1997**, *36*, 2287.
(19) Yamada, M.; Tanaka, Y.; Yoshimoto, Y.; Kuroda, S.; Shimao, I. *Bull. Chem. Soc. Jpn.* **1992**, *65*, 1006.
(20) Reger, D. L.; Grattan, T. C.; Brown, K. J.; Little, C. A.; Lamba, J. J. S.; Rheingold, A. L.; Sommer, R. D. *Organometallic Chem.* **2000**, *607*, 120.
(21) Llobet, A.; Doppelt, P.; Meyer, T. J. *Inorg. Chem.* **1988**, *27*, 514.
(22) Yam, V. W.-W.; Lo, K. K.-W.; Cheung, K.-K.; Kong, R. Y.-C. *J. Chem. Soc., Chem. Commun.* **1995**, *1191*.

no change in the spectrum for at least four titrations, indicating binding saturation had been achieved.

Syntheses. [Ru(tpm)(Cl)(dppn)]PF_6 (5). (tpm)$RuCl_3$·$3H_2O$ (0.25 g, 0.53 mmol) and dppn (0.19 g, 0.57 mmol) were heated in ethylene glycol (60 cm^3) at 120 °C for 18 h. The solution was allowed to cool, poured into methanol (150 cm^3), and filtered through celite. A saturated aqueous solution of NH_4PF_6 was added to the filtrate, causing precipitation of a brown colored solid which was collected, washed with copious amounts of water, and dried in vacuo to give a dark brown-colored solid which was purified by column chromatography on grade II neutral aluminum oxide using a mixture of 2:1 toluene/acetontrile as eluent. A dark orange-colored band containing impurities was discarded before the desired brown-colored band containing **5** was eluted. The fractions were collected and concentrated in vacuo to yield **5** (0.18 g, 38%) as a light brown-colored solid. λ_{max}(CH_3CN)/nm 206 (ϵ/dm^3 mol^{-1} cm^{-1} 30 700), 240 (32 800), 320 (72 600), 388 (9300), 409 (13 100), 443sh (10 100), and 553sh (2400); δ_H(250 MHz; CD_3CN) 6.27 (1 H, t, tpm−*H*), 6.69 (1 H, d, *J* 2.1, tpm−*H*), 6.82 (2 H, t, tpm−*H*), 7.69 (2 H, dd, *J* 3.4 and 6.7, Ar−*H*), 8.04 (2 H, dd, *J* 3.4 and 6.7, Ar−*H*), 8.32 (2 H, dd, *J* 3.4 and 6.7, Ar−*H*), 8.37 (1 H, d, *J* 2.7, tpm−*H*), 8.51 (4 H, m, tpm−*H*), 9.00 (1 H, s, tpm−*H*), 9.04 (2 H, s, Ar−*H*), 9.10 (2 H, dd, *J* 3.4 and 6.7, Ar−*H*), 9.64 (2 H, dd, *J* 3.4 and 6.7, Ar−*H*); *m*/*z* (HRMS-ES) 683.0761 (70%, [M − PF_6^-]$^+$. $C_{32}H_{22}ClN_{10}Ru$ requires 683.0794).

[Ru(tpm)(MeCN)(dppn)][PF_6]$_2$ (6). Silver trifluoromethanesulfonate (0.037 g, 0.14 mmol) and **5** (0.10 g, 0.12 mmol) were heated to reflux in acetonitrile (30 cm^3) for 8 h. The reaction was allowed to cool and filtered through celite to remove the precipitated AgCl. A saturated aqueous solution of NH_4PF_6 was added to the filtrate, causing precipitation of an orange colored solid which was collected, washed with copious amounts of water, and dried in vacuo. **6** was purified by ion-exchange column chromatography on CM25-Sephadex employing a water/acetone (5:3 v/v) solvent system containing increasing amounts of NaCl. Complex **6** was eluted as a dark red-colored band with 0.10 M NaCl. The fractions were collected and concentrated under reduced pressure. A saturated aqueous solution of NH_4PF_6 was added and the precipitate formed was collected, washed with copious amounts of water, and dried in vacuo to give **6** (0.05 g, 42%) as an orange-colored solid (Found: C, 41.5; H, 2.7; N, 15.1. $C_{34}H_{27}F_{12}N_{11}P_2Ru$·$2/3H_2O$ requires C, 41.1; H, 2.9; N, 15.5%); λ_{max}(CH_3CN)/nm 242 (ϵ/dm^3 mol^{-1} cm^{-1} 46 300), 260 (47 500), 322 (92 300), 378 (17 000), 403sh (13 800), 426sh (11 100), 477sh (6400), and 475sh (5600); δ_H(250 MHz; CD_3CN) 2.12 (3 H, s, [Ru]−C*H*$_3$CN), 6.27 (1 H, t, tpm−*H*), 6.69 (1 H, d, *J* 2.1, tpm−*H*), 6.82 (2 H, t, tpm−*H*), 7.69 (2 H, dd, *J* 3.4 and 6.7, Ar−*H*), 8.04 (2 H, dd, *J* 3.4 and 6.7, Ar−*H*), 8.32 (2 H, dd, *J* 3.4 and 6.7, Ar−*H*), 8.37 (1 H, d, *J* 2.7, tpm−*H*), 8.51 (4 H, m, tpm−*H*), 9.00 (1 H, s, tpm−*H*), 9.04 (2 H, s, Ar−*H*), 9.10 (2 H, dd, *J* 3.4 and 6.7, Ar−*H*), 9.64 (2 H, dd, *J* 3.4 and 6.7, Ar−*H*); *m*/*z* (TOF MS-ES) 834.1015 (M − PF_6, 100%).

[Ru(tpm)(py)(dppn)][PF_6]$_2$ (7). Silver trifluoromethanesulfonate (0.037 g, 0.14 mmol), pyridine (1 cm^3), and **5** (0.10 g, 0.12 mmol) were heated to reflux in acetone (30 cm^3) for 8 h. The reaction was allowed to cool and filtered through celite to remove the precipitated AgCl. A saturated aqueous solution of NH_4PF_6 was added to the filtrate, causing precipitation of an orange-colored solid which was collected, washed with copious amounts of water, and dried in vacuo. Complex **7** was purified in an identical manner to that of **6** to give **7** (0.06 g, 49%) as an orange-colored solid (Found: C, 41.6; H, 2.6; N, 14.2. $C_{37}H_{27}F_{12}N_{11}P_2Ru$·$3H_2O$ requires C, 41.5; H, 3.1; N, 14.4%); λ_{max}(CH_3CN)/nm 243 (ϵ/dm^3 mol^{-1} cm^{-1} 59 300), 259 (52 100), 322 (121 200), 399sh (21 650), 449sh (12 300), and 500sh (5500); δ_H(250 MHz; CD_3CN) 6.19 (1 H, t, tpm−*H*), 6.54 (1 H, d, *J* 2.1, tpm−*H*), 6.82 (2 H, t, tpm−*H*), 7.07 (2 H, m, py−*H*), 7.47 (2 H, m, py−*H*), 7.72−7.77 (3 H, m, 2Ar−*H* and, py−*H*), 7.99 (2 H, dd, *J* 3.4 and 6.7, Ar−*H*), 8.07 (2 H, d, *J* 3.4 and 6.7, tpm−*H*), 8.37 (3 H, m, tpm−*H* and 2Ar−*H*), 8.60 (2 H, d, tpm−*H*), 9.05 (2 H, dd, Ar−*H*), 9.13 (1 H, s, tpm−*H*), 9.14 (2 H, s, Ar−*H*), 9.72 (2 H, d, *J* 3.4 and 6.7, Ar−*H*); *m*/*z* (HRMS-ES) 872.1136 (25%, [M − PF_6^-]$^+$. $C_{37}H_{27}F_6N_{11}PRu$ requires 872.1148), 726 (20%, [M − 2PF_6^-]$^+$), 647 (25%, [M − 2PF_6^- − C_5H_5N]$^+$).

Table 1. Crystallographic Data for **[6]**·$4CH_3CN$·H_2O

empirical formula	$C_{42}H_{39}F_{12}N_{15}OP_2Ru$
M	1160.89
cryst syst	triclinic
space group	$P\bar{1}$
cryst dimens/mm^3	0.50 × 0.29 × 0.08
a/Å	11.264(2)
b/Å	12.560(3)
c/Å	18.618(4)
α/deg	84.166(4)
β/deg	79.112(4)
γ/deg	67.478(4)
U/$Å^3$	2388.1(8)
Z	2
D_c/Mg m^{-3}	1.614
F(000)	1172
M(Mo Kα)/mm^{-1}	0.495
final R1 (on *F*)	0.1075
final wR2 (on *F*)	0.3255

X-ray Crystallography. X-ray crystallographic data for **6** are summarized in Table 1. A single crystal was coated with hydrocarbon oil and attached to the tip of a glass fiber and transferred to a Bruker SMART diffractometer with an Oxford Cryosystems low-temperature system. Data were collected using graphite-monochromated Mo Kα radiation (λ = 0.71073 Å). The data were corrected for Lorentz and polarization effects. An absorption correction was applied using SADABS,[23] and structure solution and refinement were carried out using SHELXS-97 and SHELXL-97, respectively.[24,25] The structure was solved by Patterson methods and refined by full-matrix least-squares methods on F^2. Hydrogen atoms were placed geometrically and refined with a riding model, and the U_{iso} constrained to be 1.2 (1.5 for methyl groups) times U_{eq} of the carrier atom. All non-hydrogen atoms were refined anisotropically.

Results and Discussion

Synthetic Studies. The ligand dppn was prepared in a similar manner to the more widely used dppz.[22] Attempts to synthesize complex **5** in an analogous manner to the previously reported complex [Ru(tpm)(Cl)(dppz)]PF_6 (**2**) by refluxing (tpm)$RuCl_3$·$3H_2O$, dppn, and LiCl in a mixture of ethanol/H_2O were unsuccessful; this is probably due to the limited solubility of dppn in this solvent system. In contrast, reaction in ethylene glycol at 120 °C afforded an acceptable yield of complex **5**. Complexes **6** and **7** were then prepared in good yield from the parent complex **5** by removing the

(23) Sheldrick, G. M. *SADABS, A Program for Absorption Correction with the Siemens SMART Area-Detector System*; University of Göttingen: Göttingen, Germany, 1997.
(24) Sheldrick, G. M. *SHELXS-97, A Program for Automatic Solution of Crystal Structures*; University of Göttingen: Göttingen, Germany, 1997.
(25) Sheldrick, G. M. *SHELXL-97, A Program for Crystal Structure Refinement*; University of Göttingen: Göttingen, Germany, 1997.

Table 2. Selected Bond Lengths (Å) and Angles (deg) for **[6]**·$4CH_3CN·H_2O$

Ru(1)−N(1)	2.060(7)	Ru(1)−N(6)	2.060(8)
Ru(1)−N(4)	2.063(7)	Ru(1)−N(8)	2.058(7)
Ru(1)−N(5)	2.009(8)	Ru(1)−N(10)	2.044(7)
N(1)−Ru(1)−N(4)	79.2(3)	N(4)−Ru(1)−N(10)	94.0(3)
N(1)−Ru(1)−N(5)	89.9(3)	N(5)−Ru(1)−N(6)	89.9(3)
N(1)−Ru(1)−N(6)	177.4(3)	N(5)−Ru(1)−N(8)	90.8(3)
N(1)−Ru(1)−N(8)	98.5(3)	N(5)−Ru(1)−N(10)	176.1(3)
N(1)−Ru(1)−N(10)	92.7(3)	N(6)−Ru(1)−N(8)	84.1(3)
N(4)−Ru(1)−N(5)	89.3(3)	N(6)−Ru(1)−N(10)	87.7(3)
N(4)−Ru(1)−N(6)	98.2(3)	N(8)−Ru(1)−N(10)	85.9(3)
N(4)−Ru(1)−N(8)	177.7(3)		

chloride ligand with silver trifluoromethanesulfonate in either acetonitrile solution or with excess pyridine in acetone solution.

X-ray Crystallographic Study. Surprisingly, considering its structural similarity to dppz, metal complexes containing the dppn ligand are scarce in comparison to the more widely employed dppz ligand,[8,15,17,22,26−28] and there are very few structurally characterized complexes containing dppn.

Crystals of **6** suitable for a single-crystal X-ray structure analysis were grown by slow diffusion of diethyl ether into a concentrated acetonitrile solution of the complex. A summary of the crystallographic data, bond lengths, and bond angles for **6** can be found in Tables 1 and 2. An ORTEP[29] representation of the cation of **6** is shown below in Figure 3.

The coordination geometry around the ruthenium(II) center Ru(1) is best described as close to octahedral. The Ru(1)−N bond distances for the equatorial plane around Ru(1) consisting of the pyrazolyl donor atoms N(6) and N(8) of the tpm ligand [Ru(1)−N(6) = 2.060(8) Å, Ru(1)−N(8) = 2.058(7) Å] and N(1) and N(4) of the dppn ligand [Ru(1)−N(1) = 2.060(7) Å, Ru(1)−N(4) = 2.063(7) Å] are all longer than those for the corresponding axial Ru(1)−N bond distances, comprising the N(10) of the tpm ligand [Ru(1)−N(10) = 2.044(7) Å] and N(5) of the coordinated acetonitrile ligand [Ru(1)−N(5) = 2.009(8) Å]. The bite angle of the coordinated dppn ligand, 79.2(3)°, is typical of that for a five-membered chelate ring, while the bite angles of the tpm ligand [84.1(3)−87.7(3)°] are closer to the idealized 90°. To accommodate the demands of the two chelating ligands, the three trans angles involving the metal center and the nitrogen donor ligands are all slightly distorted away from the idealized 180°. Two PF_6^- anions, four acetonitrile solvent molecules, and one molecule of water, all removed for clarity in Figure 3, complete the contents of the asymmetric unit cell.

Close inspection of the unit cell contents reveals that there is extensive $\pi-\pi$ stacking between the aromatic rings of dppn ligands on neighboring cations of **6**. There are several close contacts of ca. 3.4 Å, which is comparable to the interlayer separation of the carbon sheets in graphite. Such stacking interactions have been observed before in other DNA intercalators. Expansion of the unit cell reveals that these interaction result in an infinite chain structure—Figure 4.

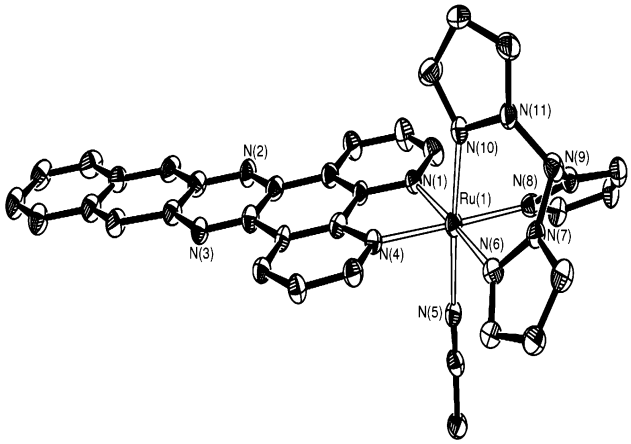

Figure 3. ORTEP[29] representation (30% probability displacement ellipsoids) of the cation of **6**. Hydrogen atoms and solvent molecules omitted for clarity.

The only other reported structure of a metal complex of dppn, $[(CO)_3Re(dppn)(py)]PF_6$, was published by Yam and colleagues.[22] The packing of $[(CO)_3Re(dppn)(py)]^+$ shows similarities to that of complex **6** with adjacent $[(CO)_3Re(dppn)(py)]^+$ units packed "head-to-tail" in the unit cell, resulting in extensive $\pi-\pi$ stacking between the aromatic rings of the dppn ligands. The distance between the ideal ring planes of the dppn ligands in this latter structure are identical to the distances found for **6**. However, the close interactions seen in the $[(CO)_3Re(dppn)(py)]PF_6$ structure do not result in the extended network seen in the structure of complex **6**.

Photophysical Studies. The photophysical properties of **2**−**7** are summarized in Tables 3 and 4. The UV−visible spectra of **2**−**7** recorded in acetonitrile solution are dominated by high-energy bands between 270 and 300 nm which correspond to $\pi \rightarrow \pi^*$ transitions of the aromatic nitrogen donor ligands. The UV−visible spectrum of the dppz ligand in acetonitrile exhibits a moderately intense band in the near-UV with two principle maxima at λ = 358 and 376 nm, which are characteristic of $\pi \rightarrow \pi^*$(dppz) transitions.[30] Consequently, the moderately intense bands in the near-UV regions for complexes **2** (351 and 367 nm), **3** (356 nm), and **4** (351 nm) are assigned to analogous transitions.

The MLCT bands for **2**−**4** all appear in the region of the spectrum typical for ruthenium(II) complexes with coordinated polyimine ligands. The bands for **3** and **4** found at 402 and 398 nm are both higher in energy than for chloride complex **2** (455 nm). The π-donor properties of the chloride ligand leads to a higher electron density on the metal center of **2** compared to **3** and **4**, resulting in the red-shift of the Ru(dπ) → dppz(π^*) ^{1}MLCT for **2**.

Complexes **5**−**7** all show a distinctive double-humped absorption which is observed at 388 and 409 nm for **5**, 378 and 403 nm for **6**, and 383 and 399 nm for **7**. The absorption

(26) Choi, S.-D.; Kim, M.-S.; Kim, S.-K.; Lincoln, P.; Tuite, E.; Nordén, B. *Biochemistry* **1997**, *36*, 214.
(27) Jiang, C.-W.; Chao, H.; Li, R.-H.; Li, H.; Ji, L.-N. *Polyhedron* **2001**, *20*, 2187.
(28) Lincoln, P.; Broo, A.; Nordén, B. *J. Am. Chem. Soc.* **1996**, *118*, 2644.
(29) Farrugia, L. J. *J. Appl. Crystallogr.* **1997**, *30*, 565.
(30) Waterland, M. R.; Gordon, K. C.; McGarvey, J. J.; Jayaweera, P. M. *J. Chem. Soc., Dalton Trans.* **1998**, *609*.

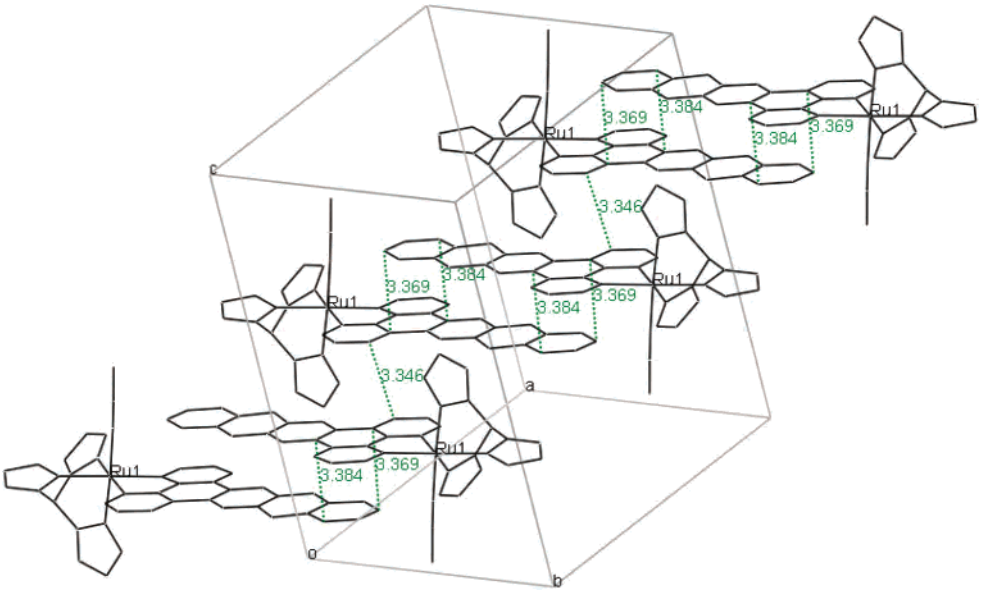

Figure 4. Structure of **6** with close contacts (Å) between the cations shown. PF_6^- anions, hydrogen atoms, and solvent molecules omitted for clarity.

Table 3. Absorption Spectra of **2**−**7** (Acetonitrile, Room Temperature)

complex	λ/nm ($10^{-3}\epsilon$/M^{-1} cm^{-1})
2	272 (58.4), 351 (14), 367 (12.5), 445 (7.9), 519sh
3	277 (55.1), 356 (13.7), 402sh, 455 (3.8)
4	277 (62.6), 312 (22.3), 351 (22.7), 398 (9.1), 484sh
5	206 (30.7), 240 (32.8), 320 (72.6), 388 (9.3), 409 (13.1), 443 (10.1), 553 (2.4)
6	242 (46.3), 260 (47.5), 322 (92.3), 378 (17), 403 (13.8), 426 (11.1), 477 (6.4)
7	243 (59.3), 259 (52.1), 322 (121), 399 (21.7), 449 (12.3), 500sh

Table 4. Luminescence Properties of $[Ru(phen)_2dppz]^{2+}$ and **2**−**7** (Acetonitrile, Room Temperature)

complex	λ_{em}/nm[a]	τ/ns[d]	ϕ[b,d]
$[Ru(phen)_2dppz]^{2+}$	607[e]	177[e]	7.3×10^{-3}[e]
2	610	−	$\sim 4.0 \times 10^{-4}$[c]
3	613	6	$\sim 7.0 \times 10^{-4}$[c]
4	656	77	2.0×10^{-3}
5	−	−	−
6	580	48	$\sim 10^{-4}$ [c]
7	600	55	$\sim 10^{-4}$ [c]

[a] λ_{ex} = 436 nm. [b] Relative quantum yields were calculated using $[Ru(bpy)_3][PF_6]_2$ in aerated acetonitrile (=0.012) as a standard. [c] Emission is very weak, leading to the estimated quantum yields. [d] Errors are ±10% for lifetime measurements and ±20% for quantum yield measurements. [e] See ref 31.

spectrum of the free dppn ligand in acetonitrile also shows a similar "double-humped" absorption in the near-UV region with maxima at λ = 390 and 411 nm. Therefore, we assign the bands in the metal complexes to analogous dppn-based transitions. Broad Ru(dπ) → dppn(π*) ^{1}MLCT bands are also observed in the visible region of the spectra for **5**−**7**. As for the analogous dppz-based systems, due to the coordination of a chloride ligand in complex **5**, the MLCT bands for **6** (477 nm) and **7** (500 nm) are both higher in energy than in **5** (550 nm). The MLCT absorptions of **5**−**7** occur at lower energies (ca. 100 nm red-shifted) than those of **2**−**4**, which is in accordance with the more extended π conjugation in the dppn ligand, cf. dppz, resulting in a stabilization of the π*(dppn)-based LUMO.

All the complexes are nonemissive in water. Excitation into the MLCT band of complexes **2**−**7** in acetonitrile solutions results in characteristic broad and unstructured emission originating from the Ru(dπ) → dppz(π*) ^{3}MLCT manifold, see Table 4. A comparison of the emission data for **2**−**4** with that of **5**−**7** reveals that, in each case, the luminescence of dppn-based system is blue-shifted compared to its dppz-based analogue. For a comparison the photophysical properties of $[Ru(phen)_2dppz]^{2+}$ are included.[31] All lifetimes were well-fit by single-exponential decays, as expected for a pure species. All complexes are weakly luminescent, with the quantum yield of emission for the dppn analogues an order of magnitude less than their dppz counterparts. Both chloride complexes **2** and **5** are almost nonemissive, and it was impossible to determine quantum yields and lifetimes accurately for **5**. Furthermore, while the quantum yield for **4** and its lifetime are of the same magnitude to $[Ru(phen)_2dppz]^{2+}$, comparable data for complex **3** are of an order of magnitude less in both parameters.

Electrochemistry. Cyclic voltammograms (CVs) of the complexes were recorded at 100 mv s^{-1} and showed good reversibility with ΔE_p < 100mV and $|E_{pc}/E_{pa}| = 1$, unless otherwise stated—Figure 5 below shows details of the CVs for the new complexes **5**−**7**.

Complexes **2**−**7** display one reversible oxidation associated with the ruthenium(III)/(II) couple and several reversible or irreversible processes related to the dppz ligand or dppn ligand—Table 5. The value of $E_{1/2}$ varies by nearly 580 mV between the six complexes. The potential of the ruthenium(III)/(II) couple shows little variation upon replacing the ligand dppz with dppn; dppz-based complexes **2**−**4** have similar $E_{1/2}$ values to their corresponding dppn-based complexes **5**−**7**. However, $E_{1/2}$ values of the ruthenium(III)/(II) couple is highly dependent upon the nature of the axial ligand in the complexes **2**−**7**: when the axial ligand is chloride

(31) Nair, R. B.; Cullum, B. M.; Murphy, C. J. *Inorg. Chem.* **1997**, *36*, 962.

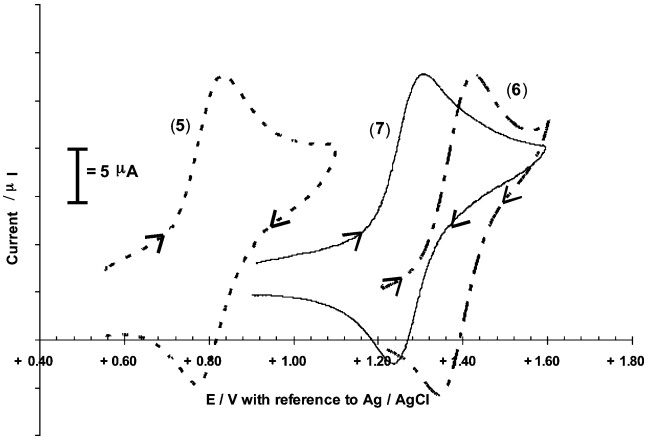

Figure 5. Electrochemical CV (current vs voltage) for complexes **5**−**7**.

Table 5. Electrochemical Data for **2**−**7**[a]

complex	metal-based oxidations $E_{1/2}$/V	ligand-based reductions $E_{1/2}$/V
2	+0.89	−0.91
3	+1.36	−0.86, −1.29,[b] −1.67[b]
4	+1.30	−0.87, −1.24[b]
5	+0.80	−0.82, −1.49,[b] −1.81[b]
6	+1.38	−0.76, −1.41
7	+1.28	−1.18, −1.41, −1.63

[a] Conditions: vs Ag/AgCl, CH_3CN, 0.1 M [^{t}NBu$_4$]PF_6, under N_2, 25 °C. [b] Reductions are not fully chemically reversible, only $E_{p,c}$ values are quoted.

the ruthenium(III)/(II) couple occurs at +0.89 (complex **2**) and +0.80 V (complex **5**), for pyridine the ruthenium(III)/(II) couple occurs at +1.30 (complex **4**) and +1.28 V (complex **7**), and finally when the ligand is acetonitrile the ruthenium(III)/(II) couple occurs at +1.36 (complex **3**) and +1.38 V (complex **6**). Previous studies on nonintercalating Ru^{II} complexes has demonstrated that such behavior can be rationalized by considering the σ- and π-donor and acceptor characteristics of coordinating ligands. In this case, the effects are solely attributable to the nature of the monodentate axial ligand.

Chloride is a good σ-donor and a good π-donor, so it effectively has an induction effect pushing electrons onto the ruthenium(II) center and destabilizing the ruthenium(II) oxidation state, at the same time stabilizing the ruthenium(III) oxidation state; therefore, the complex is relatively easy to oxidize. Pyridine is a good σ-donor ligand but is also a good π-acceptor, which means there is some delocalization of the 4d electrons off the ruthenium(II) center onto the pyridine. This has the effect of stabilizing the ruthenium(II) oxidation state with respect to the ruthenium(III) oxidation state and making the oxidation process more difficult. Nitriles as ligands are poorer σ-donors and better π-acceptors than pyridines, so the ruthenium(II) oxidation state is stabilized relative to the ruthenium(III) oxidation state even more, resulting in the ruthenium(III)/(II) couple being slightly more anodic than for the pyridine complex.

Characteristic ligand-centered reductions are also seen for each of the complexes. The first of these waves is reversible in each compound; however, subsequent waves are mostly irreversible (see Table 5). The ligands dppz and dppn are more readily reduced than other diimine ligands such as phen and bpy due to the lower-lying π^* orbital of the phenazine moiety. Thus the π-accepting site in dppz and dppn is localized on the phenazine portion of the ligands.[33−36] This makes any electrochemical and photochemical processes involving this orbital very sensitive to its surroundings.

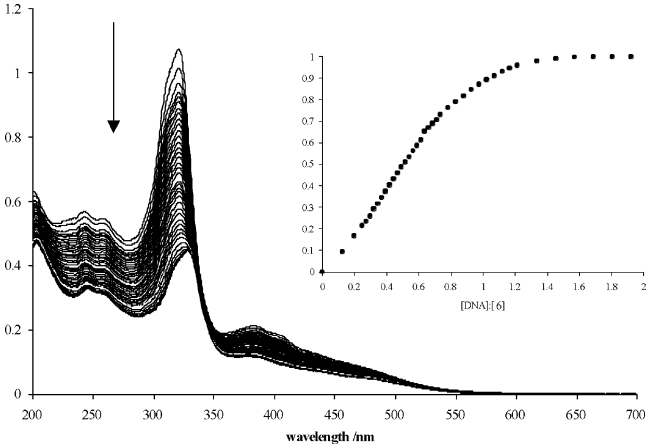

Figure 6. Electronic spectral trace of [**6**]Cl_2 in buffer (25 mM NaCl, 5 mmol tris, pH 7.0) upon addition of double-stranded CT-DNA. Inset: Binding curve for [**6**]Cl_2.

DNA Binding Studies. Electronic Absorption Titrations. Water-soluble chloride salts of **2**−**4**, **6**, and **7** were obtained via anion metathesis of their respective PF_6^- salts using [nBu$_4$N]Cl in acetone. While [**2**]Cl displays relatively good water solubility, the chloride salt of complex **5** is not sufficiently soluble in aqueous buffer for its DNA binding properties to be investigated.

In contrast to **3** and **4**, there was no detectable "light switch" effect observed upon addition of CT-DNA to aqueous solutions of [**2**]Cl, [**6**]Cl_2, and [**7**]Cl_2. Therefore, the interaction of the monocation [**2**]Cl, and dications [**6**]Cl_2 and [**7**]Cl_2 with CT-DNA in aqueous buffer (25 mM NaCl, 5 mmol tris, pH 7.0) was investigated using UV−visible spectroscopic titrations and compared to the data obtained for **3** and **4,** reported in a preliminary communication. Addition of CT-DNA to solutions of the complexes results in characteristically large hypochromicity in both MLCT and $\pi \rightarrow \pi^*$ absorption bands. For [**6**]Cl_2 there is an appreciable bathochromic shift of one of the high-energy bands from 320 to 328 nm, see Figure 6. The raw data

(32) See for example: Juris, A; Balzani, V; Barigelletti, Campagna, S; Belser, P; von Zelewsky, A. *Coord. Chem. Rev.* **1988**, *84*, 85. Coe, B. J.; Meyer, T. J.; White, P. S. *Inorg. Chem.* **1993**, *32*, 4012. Anderson, P. A.; Deacon, G. B.; Haarmann, K. H.; Keene, F. R.; Meyer, T. J.; Reitsma; Skelton, B. W.; Strouse, G. F.; Thomas, N. C.; Treadway, J. A.; White, A. H. *Inorg. Chem.* **1995**, *34*, 6145 and references therein.
(33) Ackermann, M. N.; Interrante, L. V. *Inorg. Chem.* **1984**, *23*, 3904.
(34) Amouyal, E.; Homsi, A.; Chambron, J.-C.; Sauvage, J.-P. *J. Chem. Soc., Dalton Trans.* **1990**, *1841*.
(35) Chambron, J.-C.; Sauvage, J.-P.; Amouyal, E.; Koffi, P. *New J. Chem.* **1985**, *9*, 527.
(36) Fees, J.; Kaim, W.; Moscherosch, M.; Matheis, W.; Klíma, J.; Krejčík, M.; Záliš, S. *Inorg. Chem.* **1993**, *32*, 166.
(37) Nordén, B.; Lincoln, P.; Akerman, B.; Tuite, E. In *Metal Ions in Biological Systems*; Sigel, H., Sigel, A., Eds.; Marcel Dekker: New York, 1996; Vol. 33, p 177.
(38) Satyanarayana, S.; Dabrowiak, J. C.; Chaires, J. B. *Biochemistry* **1992**, *31*, 9319.

Table 6. Selected Binding Parameters For [**2**]Cl, [**3**]Cl_2, [**4**]Cl_2, [**6**]Cl_2, and [**7**]Cl_2 with CT-DNA

complex	K_b dm^3 mol^{-1}	site size *S*
[**2**]Cl	3.8×10^5	2.5
[**3**]Cl_2	4.9×10^6	2.9
[**4**]Cl_2	5.2×10^6	3.4
[**6**]Cl_2	2.4×10^6	1.6
[**7**]Cl_2	1.9×10^6	1.5

Table 7. Selected Binding Parameters for [**4**]Cl_2, [**6**]Cl_2, and [**7**]Cl_2 with Synthetic Oligonucleotides

	poly(dA)·poly(dT)		poly(dG)·poly(dC)	
complex	K_b dm^3 mol^{-1}	site size *S*	K_b dm^3 mol^{-1}	site size *S*
[**4**]Cl_2	1.5×10^{5a}	2.7[a]	1.1×10^{6a}	2.8[a]
[**6**]Cl_2	4.0×10^6	1.4	2.0×10^6	1.0
[**7**]Cl_2	2.0×10^6	1.4	5.0×10^5	1.0

[a] Determined by isothermal titration calorimetry (ITC), see ref 16.

produced typical saturation binding curves (see inset Figure 6). Although higher binding ratios were investigated, further aliquots of DNA produced no additional changes in the absorption spectra of the complexes

Fits of data to the McGhee−Von Hippel (MVH) model,[39] Table 6, indicate that [**6**]Cl_2 ($K_b = 2.4 \times 10^6$ dm^3 mol^{-1} and a site size $S = 1.6$) has a similar binding affinity to [**7**]Cl_2 ($K_b = 1.9 \times 10^6$ dm^3 mol^{-1}, $S = 1.5$). The binding parameters are entirely comparable to those obtained for $[(phen)_2Ru(dppz)]^{2+}$ (3.2×10^6 and 1.7×10^6 dm^3 mol^{-1} for the Δ and Λ enantiomers, respectively)[11] and those obtained previously for [**3**]Cl_2 and [**4**]Cl_2.[5] Interestingly, [**2**]-Cl displays an order of magnitude lower binding affinity (3.8×10^5 dm^3 mol^{-1}, $S = 2.5$).

The above observations and binding parameters are consistent with the interaction of a metallo-intercalator and DNA.[1,7,14,15,37] The observation of large hypochromicity is suggestive, but not definitive, proof of an intercalative DNA binding mode for the complexes. One simple method for authoritatively distinguishing an intercalative binding mode is viscometry. Classical intercalation results in a lengthening of DNA, thus producing a concomitant increase in the relative specific viscosity of aqueous DNA solutions.[38] The relative specific viscosity of CT-DNA significantly increases upon addition of [**6**]Cl_2 and [**7**]Cl_2—Figure 7. Such an observation is a priori evidence for an intercalative binding mode of [**6**]Cl_2 and [**7**]Cl_2 to CT-DNA.

Synthetic DNA Binding. In order to gain more insight into the possibility of preferential binding of [**6**]Cl_2 and [**7**]-Cl_2 with DNA, UV−visible absorption titrations using the synthetic oligonucleotides poly(dA)·poly(dT) and poly(dG)·poly(dC) were performed. As was observed for the interaction of [**6**]Cl_2 and [**7**]Cl_2 with CT-DNA, the band at ca. 320 nm in the UV−visible spectra of [**6**]Cl_2 and [**7**]Cl_2 displays hypochroism and a small red-shift in the presence of synthetic oligonucleotides. An example of the interaction of [**6**]Cl_2 with poly(dA)·poly(dT) is shown below in Figure 8 and the relevant binding parameters are summarized in Table 7.

(39) McGhee, J. D.; von Hippel, P. H. *J. Mol. Biol.* **1974**, *86*, 469.

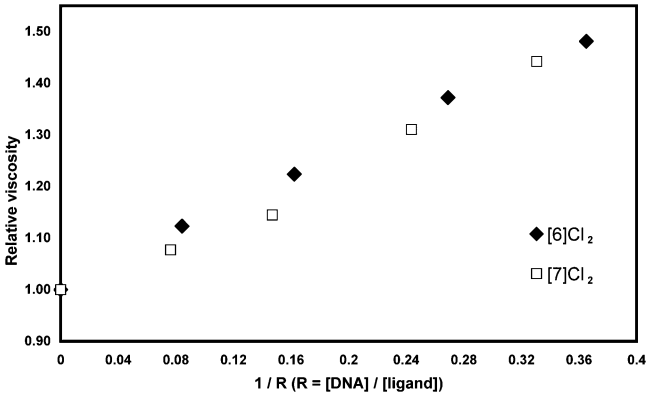

Figure 7. Changes in the relative viscosity $(\eta/\eta^\circ)^{1/3}$ of an aqueous CT-DNA solution on addition of complexes [**6**]Cl_2 and [**7**]Cl_2.

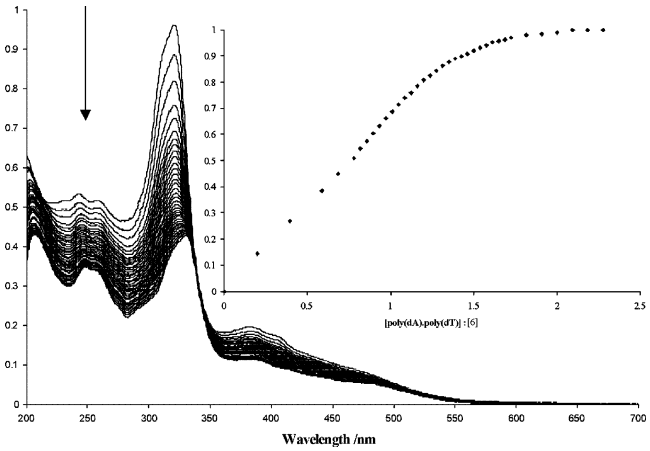

Figure 8. Absorption titration of [**6**] and poly(dA)·poly(dT). Inset: Binding curve for [**6**]Cl_2.

Discussion

Our study here represents the first *quantitative* investigation of the binding parameters of ruthenium(II) complexes of dppn with CT-DNA and synthetic oligonucleotides and also offers insight into the contribution of electrostatics toward metallo-intercalator binding. Since the shape and size of [**2**]Cl, [**3**]Cl_2, and [**4**]Cl_2 are almost identical, the increased binding affinity of [**3**]Cl_2 and [**4**]Cl_2 over [**2**]Cl for CT-DNA must be due to enhanced electrostatic interactions between the dications of [**3**]Cl_2 or [**4**]Cl_2 and the polyanionic DNA. The site sizes (*S*) for [**2**]Cl, [**3**]Cl_2 and [**4**]Cl_2 are ca. three base-pairs, which is consistent with values reported for many other intercalators. Unfortunately, it was not possible to determine binding parameters for the interaction of the monocationic dppn complex [**5**]Cl with CT-DNA, which was due to low solubility of [**5**]Cl in tris buffer. However, on the basis of electrostatic interactions as discussed above for [**2**]Cl compared to [**3**]Cl_2 and [**4**]Cl_2, the binding constants for [**5**]Cl with CT-DNA and synthetic oligonucleotides is expected to be an order of magnitude less than [**6**]Cl_2 or [**7**]Cl_2.

The intrinsic binding constants for the interaction of [**6**]-Cl_2 and [**7**]Cl_2 with CT-DNA are of the same magnitude as for the dppz-based complexes [**3**]Cl_2 and [**4**]Cl_2. Clearly, the increase in potential intercalative area on moving from dppz to dppn does not lead to a concomitant increase in binding

affinity. However, studies involving the higher-binding-affinity complexes and synthetic oligonucleotides reveal an interesting trend. While previous studies have revealed that, thanks to specific interactions involving ancillary ligands, the dppz-based complex [**4**]Cl_2 binds with an order of magnitude preference to poly(dG)·poly(dC), [**6**]Cl_2 and [**7**]-Cl_2 show a much less pronounced preference for poly(dA)·poly(dT). This latter observation is consistent with previous studies[5,7,8] on dppz-based complexes such as $[Ru(phen)_2(dppz)]^{2+}$ and $[Re(CO)_3(py)(dppz)]^{+}$, where it has been suggested that flexible A−T tracks can accommodate the steric demand of the ancillary ligands of metallo-intercalator more easily than the deeper more rigid GC rich sequences.

Clearly, the replacement of dppz with dppn does not lead to an increase in binding affinity but leads to the loss of the specific contacts observed for [**4**]Cl_2. This indicates that the more extended dppn ligand does not lead to an increase in the overlap of the metal complex intercalative surface with DNA base pairs and suggests that in dppn-based complexes the ruthenium(II) metal center and its coordinated ancillary ligands are held at a distance and/or angle that prevents specific interactions with the groove of the duplex. Thus, nonspecific steric interactions dominate resulting in the previously observed preference for AT tracks.

Complexes **5**−**7** show strikingly different photophysical properties compared to **2**−**4**, with quantum yields and lifetimes being lower for the dppn-based complexes compared to their dppz analogues. It is tempting to conclude that these observations are a direct consequence of more extended delocalization in dppn compared to dppz leading to a smaller HOMO−LUMO gap. Thus, the emission properties of the dppn complexes would be entirely explained by energy gap law arguments.[40] However, in monaqueous solvents, we observe a blue-shift in the luminescence of **5** and **7**, compared to **2** and **4**, thus contradicting this conclusion. Alternatively, it is known that the luminescence of Ru^{II} systems can involve several possible excited states. For example, for the $[Ru(bpy)_2(dppz)]$ system, the light-switch effect is due to subtle interplay between a ^{3}MLCT emissive excited state, analogous to that found in $[Ru(bpy)_3]$, and a dark excited-state centered on the phenazine unit of dppz. It is possible that the reduced luminescence of [Ru(dppn)] systems is due to a related dark state. Studies to investigate this question are underway.

(40) Casper, J. V; Kober, E. M.; Sullivan, B. P.; Meyer, T. J. *J. Am. Chem. Soc.* **1982**, *104*, 630. Kober, E. M.; Casper, J. V.; Lumpkin, R. S.; Meyer, T. J. *J. Phys. Chem.* **1986**, *90*, 3722

Conclusions

A series of tris(1-pyrazolyl)methane ruthenium(II) complexes containing the dppn ligand have been synthesized, and complex **6** has been characterized by single-crystal X-ray diffraction.

For the first time the DNA binding properties of a [Ru(dppz)] monocation has been investigated. It was found that the monocation [**2**]Cl bound to DNA with an affinity that is an order of magnitude lower than that of analogous dications, confirming that electrostatic effects contribute significantly to the binding affinity of this class of metallo-intercalators.

Studies on the interaction of [**6**]Cl_2 and [**7**]Cl_2 with CT-DNA, poly(dA)·poly(dT), and poly(dG)·poly(dC) revealed that while affinities are comparable to those previously determined for [Ru(tpm)(dppz)] based complexes, binding preferences are reversed, with a small preference for AT sequences being observed. In future work, more detailed studies will be employed to further delineate the thermodynamic parameters for the above binding processes and the photophysics of this class of metallo-intercalators.

Acknowledgment. We gratefully acknowledge the support of EPSRC (C.M.) and BBSRC (S.P.F., M.W., and J.A.T).

Supporting Information Available: Crystallographic data file for complex **6** in CIF format. This material is available free of charge via the Internet at http://pubs.acs.org.

IC0607134